

Hall and Ion Slip Influence on Unsteady MHD Convective Rotating Flow of Non-Newtonian Fluid through Porous Medium with Chemical Reaction

R.Vijaya Kumar¹ and A. Jancy Rani²

¹Mathematics Section, Faculty of Engineering and Technology, Annamalai University, Annamalai Nagar,

Chidambaram, Tamilnadu - 608 002,

Department of Mathematics, Periyar Arts College, Cuddalore,

Tamilnadu – 608 002, India.

²Research Scholar, Department of Mathematics, Annamalai University, Annamalai Nagar, Chidambaram, Tamilnadu - 608 002, India

Abstract: The purpose of this study is to investigate the effects of Hall and ion slip on the unsteady MHD convective rotating flow of Casson fluid through porous media under the impact of chemical reaction. The equations governing flow, heat, and mass transport may be reduced to a set of ordinary differential equations that can be solved analytically by utilizing the perturbation technique. The numerical values of shear stress, Nusselt number, and Sherwood number at the plate are tabulated, while the changes in fluid velocity, temperature, and concentration fields caused by changes in different physical parameters are visually shown.

Keywords: Casson fluid; Hall and ion slip effect; Perturbation method; Magnetohydrodynamic (MHD); Porous medium; Rotating flow.

1. Introduction

One of the rheologic and fluid dynamic property of blood flow deals a substantial bit part in the essential grasping and treating of many cardiovascular, cerebra vascular and arterial diseases. Many research scholars are making serious attempt to do research in blood. Blood is plasma, platelets, erythrocytes and other particles. Rheologic ally blood flow behaves differently in large blood vessels and narrow blood vessels. It behaves homogenous Newtonian fluid way in large blood vessels and non-Newtonian in narrow blood vessels e.g., capillaries. The flow behaviour is further intricated due to the fact that at low shear rate certain chemical reactions occur that may cause momentous changes in the flow behaviour of blood. Since harmful experiments cannot be carried out on living human beings, many theoretical researchers experiment blood flow through human artery with a branch capillary. The complications in describing the flow of blood in the arterial system leads to develop a constitutive mathematical model that can explain its non-Newtonian behaviour[1]. Craig and Watson supposed, since blood is an electrically conducting fluid, it exhibits magnetohydrodynamic (MHD) property, which may cause potential health consequences. When a magnetic field is applied to a moving, electrically conducting fluid, electric and magnetic fields are generated. They interact and create Lorentz force, which is a body force per unit volume. It has a substantial influence on preventing liquid movement[2]. Ajaz explains the complexities of blood flow via a nonsymmetric horizontal artery with a slight stenosis. It is classified as a micropolar fluid that is homogenous and incompressible. The impact of rotation and magnetic field was studied in detail and numerically estimated [3]. Ali and others study the use of magnetic particles for medicinal purposes in a brief manner. Their blood flow analysis uses a concealed magnetic field that is administered perpendicularly. As a result, adequate utilisation of magnetic field strength can regulate particle and blood mobility [4]. Saqib and others experimented the blood flow through a cylindrical tube [5]. Ramakrishnan proposed simplified mathematical model to understand the behaviour of blood flow through porous medium with finite thickness [6].

Shehzad and others (Shehzad et al., 2013) did their research in the flow of electrically conducting Casson fluid through a porous stretching sheet by the influence of mass transfer with the chemical reaction. Hussanan[8] investigated unsteady motion in the boundary layer on MHD flow of a Casson fluid inserting through a oscillating vertical plate with the effect of heat. A significant result found and acquired exact solutions. Khalid [9] research is in two-fold, those are MHD and porous medium. The magnetic fields induce currents in the fluid flow of a transient phenomenon that past in an oscillating vertical plate thrust in a porous medium with constant wall temperature and used Laplace technique to find results. The investigation of boundary layer flow on MHD incompressible Casson fluid past in the porous medium is explored by Shehzad(Shehzad et al.,2016). Biswas and others[11]discussed heat and mass transfer of Casson fluid on electrically conducting through a vertical plate with emission of

energy and chemical reaction. Hussanan[12]investigated the heat transfer effect on the unsteady boundary layer flow of a Casson fluid past an infinite oscillating vertical plate with Newtonian heating.

Abro & Khan[13]demonstrated the effects of the fractional calculus derivative without singular Kernel on the double convection MHD flow of a Casson fluid. They projected the effects by using and non-using magnetic field and a porous medium over an oscillating vertical plate. The author Pattnaik[14]highlights the novelty of analyzing the effect of angle of inclination on the flow phenomena with the help of heat source / sink and destructive reaction. Saqib[15]calculated the slip effect at the boundary of a vertical plate from the flow of Casson fluid with the help of radiative heat and mass transfer utilizing the first order chemical reaction. Veera Krishna [16]analyzed the unsteady MHD oscillatory free convective flow of second grade fluid through porous media between two vertical plates is subjected to Hall effects. Khan[17]scrutinized and presented on magnetohydrodynamic (MHD) natural convection flow over a moving plate on combined effects of heat generation and chemical reaction inserted in a porous medium. Rajakumar[18] investigated hall and ion slip current on unsteady, free convective, magnetohydrodynamic Casson fluid flow passes through semi – infinite oscillatory vertical porous plate with time dependent permeability. Jha & Sarki[19] did a theoretical analysis using Defour effects and first order chemical reaction with the moving porous infinite vertical plate transferring mass and free convection, fully developed, steady motion are taken into the account. Kumar & Vishwanath[20] analyzed MHD viscoelastic fluid, free convective flow passes in a porous regime into the channel of inclined with the effect of hall and ion slip. Makhalemele(Makhalemele et al., 2020) examined incompressible viscous electrically conducting mixed convective flow over a two phase system consisting of elastic solid and incompressible fluid phase. The channel plates are activated by both buoyancy force and oscillatory pressure gradient.

In recent years the author Singh & Seth s [22], Krishna & Chamkha,[23], Krishna[24], Krishna, Sravanthi[25], Krishna & Chamkha[26], (Krishna, Ahamad[27], Krishna[28], Dharmiah, Sridhar, Balamurugan, & Kala[29] who have made an attempt to deal with hall and ion-slip effect on magnetohydrodynamics over a vertical surface, penetrable semi-infinite moving plate, infinite vertical porous plate, rigidly rotating parallel plates, semi-infinite absorbent plate with rotation and kinds of Newtonian and non-Newtonian fluids applied in the porous materials are quite admirable. Veera Krishna [30]invesgated various articles regarding hall and ion slip effect on MHD. But in this paper on double – diffusive unsteady natural convective MHD rotating flow in the micro – polar fluid through vertical moving plate. Analyzing the literature above-mentioned, new research is established. The main objective of this research is to investigate hall and ion slip on the blood flow distributing magnetic particles uniformly passes into porous material with chemical reaction in a channel. In addition, in the magnetic field blood flow is in rotation. Perturbation technique utilized to get exact solution. Various parameters impact is shown in several graphs.

2. Mathematical method and solution

Convective flow in two infinite plates at distance z_0 , instituted in a soaked porous medium by the influence of invariable transverse magnetic field of strength B_0 and the impact of angle of inclination is scrutinized. The fluid is applied at a uniform angular velocity around the normal to the plate along the x - and z - axes, which are perpendicular to the plates and are the rigid rotation axes, as shown in Fig. 1. The temperature and concentration of the plate and the surrounding fluid are assumed to be the same. The magnetic

Reynolds number is taken into account while controlling velocities. The plates of the channel occupying the planes $z = \pm \frac{z_0}{2}$ are of infinite extent and all the physical quantities depend upon z and t .

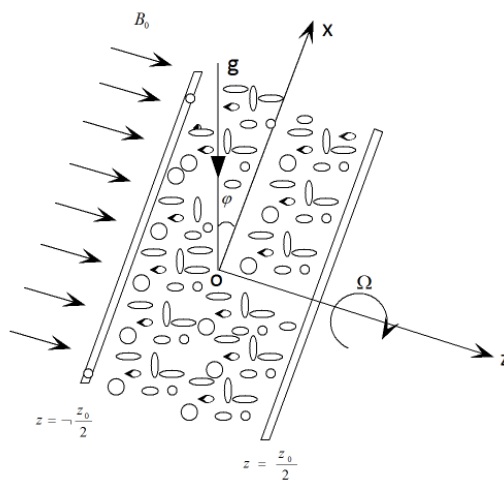


Fig. 1 Physical model of the problem

For an isotropic and incompressible Casson fluid flow, the rheological equation of state is [31]

$$\tau_{ij} = \begin{cases} 2\left(\mu_B + \frac{p_y}{\sqrt{2\pi}}\right)e_{ij}, \pi > \pi_c \\ 2\left(\mu_B + \frac{p_y}{\sqrt{2\pi_c}}\right)e_{ij}, \pi < \pi_c \end{cases} \quad (1)$$

Where, $\tau_{ij} - (i, j)^{th}$, $\pi = e_{ij}e_{ij}$, $e_{ij} - (i, j)^{th}$, μ_B , p_y , π_c are component of the stress tensor, component of the deformation tensor, product of the deformation rate components with itself, yield stress and critical value of this product based on the non-Newtonian model

The governing equations for the flow are given by [32].

$$\frac{\partial w}{\partial z} = 0 \quad (2)$$

$$\frac{\partial u}{\partial t'} - 2\Omega v = \nu \left(1 + \frac{1}{\beta_c}\right) \frac{\partial^2 u}{\partial z'^2} + \frac{B_0 J_y}{\rho} - \frac{\nu}{k'} u + g\beta_T(T - T_1)\cos\phi + g\beta_C(C - C_1)\cos\phi \quad (3)$$

$$\frac{\partial v}{\partial t'} + 2\Omega u = \nu \left(1 + \frac{1}{\beta_c}\right) \frac{\partial^2 v}{\partial z'^2} - \frac{B_0 J_x}{\rho} - \frac{\nu}{k'} v \quad (4)$$

$$\rho C_p \frac{\partial T}{\partial t'} = K_T \frac{\partial^2 T}{\partial z'^2} - \frac{\partial q_r}{\partial z'} - Q_0(T - T_1) \quad (5)$$

$$\frac{\partial C}{\partial t'} = D \frac{\partial^2 C}{\partial z'^2} - k_c(C - C_1) \quad (6)$$

where, u and v are the components of velocities along x and y directions, respectively, $\beta_c = \mu_B \sqrt{2\pi_c} / p_y$ - non-Newtonian Casson parameter, t' - the time, ρ - the fluid density, ν - the kinematic viscosity, g - the acceleration due to gravity, β_T and β_C - the thermal and concentration expansion coefficients respectively, k' - the permeability of the porous medium, B_0 - the magnetic induction, T - the temperature, K_T - thermal diffusivity of fluids, C_p - specific heat at constant pressure, q_r - the radioactive heat flux, C - the concentration, D - the coefficient of chemical molecular diffusivity, k_c - chemical reaction, T_1 and C_1 are the temperature and concentration.

The following are the initial and boundary conditions:

$$\left. \begin{aligned} t < 0, u = 0, v = 0, T = T_1, C = C_1 \quad \forall z, \\ t > 0, \frac{\partial u}{\partial z'} = \frac{\alpha}{\sqrt{k_0}} u, v = 0, T = T_2 + \varepsilon^{i\omega t}(T_2 - T_1), C = C_2 + \varepsilon^{i\omega t}(C_2 - C_1), \text{ at } z' = \frac{z_0}{2} \\ \frac{\partial u}{\partial z'} = \frac{\alpha}{\sqrt{k_0}} u, v = 0, T = T_1, C = C_1, \text{ at } z' = -\frac{z_0}{2} \end{aligned} \right\} \quad (7)$$

For optically thin fluids, the radiative heat flow [33], [14], [34] is give by

$$\frac{\partial q_r}{\partial z'} = -4I(T - T_1) \quad (8)$$

$$\text{and } I = \int_0^\infty (K_\lambda)_w \left(\frac{\partial e_{\lambda h}}{\partial T^*} \right)_w d\lambda \quad (9)$$

We derive (5) by using Eq. (8) in (5).

$$\rho C_p \frac{\partial T}{\partial t'} = K_T \frac{\partial^2 T}{\partial z'^2} - 4I(T - T_1) - Q_0(T - T_1) \quad (10)$$

Hall and ion slip currents should be examined since electron-atom collisions are believed to occur often. As a result, the velocity in the y-direction is determined by the Hall and ion slip currents. The generalised Ohm's law is modified to incorporate the Hall and ion slip effects when the magnetic field is sufficiently high [35], [36],[34], and [40].

$$J = \sigma'(E + q \times B) - \frac{\beta_e}{B_0}(J \times B) + \frac{\beta_e \beta_i}{B_0^2}((J \times B) \times B) \quad (11)$$

where \mathbf{q} , \mathbf{B} , \mathbf{E} , \mathbf{J} , σ' , α_e , α_i are the velocity vector, magnetic field vector, electric field vector, current density vector, effective electric conductivity of hybrid blood, Hall parameter, and ion slip parameter, respectively.

The Maxwell equations are as [39]:

$$\nabla \times E = -\frac{\partial B}{\partial t}, \nabla \cdot B = 0, \nabla \cdot J = 0$$

The electron pressure gradient and thermoelectric effects are ignored. Eq. (11) reduces under these assumptions.

$$(1 + \alpha_i \alpha_e) J_x + \alpha_e J_z = \sigma' B_0 v \quad (12)$$

$$(1 + \alpha_i \alpha_e) J_z - \alpha_e J_x = -\sigma' B_0 u \quad (13)$$

We get by solving Eqs. (12) and (13)

$$J_x = \sigma' B_0 (\beta_{I1} u + \beta_{I2} v) \quad (14)$$

$$J_z = -\sigma' B_0 (\beta_{II1} v - \beta_{II2} u) \quad (15)$$

$$\text{where, } \beta_I = \frac{1 + \alpha_e \alpha_i}{(1 + \alpha_e \alpha_i)^2 + \alpha_e^2}, \beta_{II} = \frac{\alpha_e}{(1 + \alpha_e \alpha_i)^2 + \alpha_e^2}$$

Substituting Eqs. (14) and (15) into (3) and (4), respectively, yields (3) and (4).

$$\frac{\partial u}{\partial t} - 2\Omega v = \nu \left(1 + \frac{1}{\beta_c} \right) \frac{\partial^2 u}{\partial z^2} + \frac{\sigma B_0^2 (\beta_{I2} v - \beta_{II2} u)}{\rho} - \frac{\nu}{k'} u + g\beta_T (T - T_1) \cos \varphi + g\beta_c (C - C_1) \cos \varphi \quad (16)$$

$$\frac{\partial v}{\partial t} + 2\Omega u = \nu \left(1 + \frac{1}{\beta_c} \right) \frac{\partial^2 v}{\partial z^2} - \frac{\sigma B_0^2 (\beta_{I1} u + \beta_{II1} v)}{\rho} - \frac{\nu}{k'} v \quad (17)$$

Combing the equations (16) and (17), we get in the form of $q' = u + iv$

$$\frac{\partial q'}{\partial t} + 2i\Omega q' = \nu \left(1 + \frac{1}{\beta_c} \right) \frac{\partial^2 q'}{\partial z^2} - \frac{\sigma B_0^2 (\beta_I + i\beta_{II})}{\rho} q' - \frac{\nu}{k'} q' + g\beta_T (T - T_1) \cos \varphi + g\beta_c (C - C_1) \cos \varphi \quad (18)$$

To make the governing equations easier to understand, the following non-dimensional variables are defined.

$$z = \frac{z'}{z_0}, q = \frac{q'}{q_0}, t = \frac{t' q_0}{z_0}, a = \frac{\tilde{a} z_0}{q_0}, \theta = \frac{T - T_1}{T_2 - T_1}, \varphi = \frac{C - C_1}{C_2 - C_1},$$

The non-dimensional form of governing equations reduces Eqs. (6),(7),(10) and (18) is as follows:

$$\text{Re} \frac{\partial q}{\partial t} = \left(1 + \frac{1}{\beta_c} \right) \frac{\partial^2 q}{\partial z^2} - (M^2 (\beta_I + i\beta_{II}) + 2iR + \sigma^2) q + Gr \theta \cos \varphi + Gm \phi \cos \varphi \quad (19)$$

$$\text{Re} \frac{\partial \theta}{\partial t} = \frac{1}{\text{Pr}} \frac{\partial^2 \theta}{\partial z^2} - N \theta \quad (20)$$

$$\text{Re} \frac{\partial \phi}{\partial t} = \frac{1}{\text{Sc}} \frac{\partial^2 \phi}{\partial z^2} - K_c \phi \quad (21)$$

where, $Gr = \frac{g\beta_T z_0^2 (T_2 - T_1)}{\nu q_0}$ is the thermal Grashof number, $Gm = \frac{g\beta_C z_0^2 (C_2 - C_1)}{\nu q_0}$ is the mass Grashof number,

$M = \frac{\sigma B_0^2 z_0^2}{\nu \rho}$ is the squared Hartmann number, $K_c = \frac{z_0^2 k_c}{\nu}$ is the chemical reaction parameter, $Pr = \frac{\rho C_p \nu}{K_T}$ is the Prandtl

number, $Sc = \frac{\nu}{D}$ is the Schmidt number, $R = \frac{\Omega z_0^2}{\nu}$ is the rotation parameter and $Re = \frac{q_0 z_0}{\nu}$ is the Reynolds number.

The non-dimensional boundary conditions are as follows:

$$\left. \begin{aligned} t < 0, q = 0, \theta = 0, \phi = 0 \quad \forall z, \\ t > 0, \frac{\partial q}{\partial z} = \alpha \sigma q, \theta = 1 + \varepsilon^{i\omega t}, \phi = 1 + \varepsilon^{i\omega t}, \quad \text{at } z = \frac{1}{2} \\ \frac{\partial q}{\partial z} = \alpha \sigma q, \theta = 0, \phi = 0, \quad \text{at } z = -\frac{1}{2} \end{aligned} \right\} \quad (22)$$

where, $\sigma = \frac{z_0}{\sqrt{k_0}}$ is the porous parameter, $N = \zeta_1 + \zeta_2$ is the resultant of thermal radiation parameter and heat source/sink

parameter, $\zeta_1 = \frac{4I z_0^2}{\rho C_p \nu}, \zeta_2 = \frac{Q_0 z_0^2}{\rho C_p \nu}$

3. Solution of the problem

The fluid velocity, temperature, and concentration are assumed to be as follows in order to solve the corresponding equations (19)-(21), yield

$$\left. \begin{aligned} q(z, t) &= q_0(z) + \varepsilon e^{i\omega t} u_1(z) + O(\varepsilon^2), \\ \theta(z, t) &= \theta_0(z) + \varepsilon e^{i\omega t} \theta_1(z) + O(\varepsilon^2), \\ \phi(z, t) &= \phi_0(z) + \varepsilon e^{i\omega t} \phi_1(z) + O(\varepsilon^2) \end{aligned} \right\} \quad (23)$$

We get the following set of differential equations $q_0, q_1, \theta_0, \theta_1, \phi_0, \phi_1$ by substituting Equations (23) into Equations (19) to (22).

We omit the higher order of ε^2 and simplify.

Zeroth order equations:

$$q_{0zz} - l_3 q_0 + l_4 \theta_0 + l_5 \phi_0 = 0 \quad (24)$$

$$\theta_{0zz} - l_9 \theta_0 = 0 \quad (25)$$

$$\phi_{0zz} - l_{11} \phi_0 = 0 \quad (26)$$

First-order equations:

$$q_{1zz} - l_6 q_1 + l_7 \theta_1 + l_8 \phi_1 = 0 \quad (27)$$

$$\theta_{1zz} - l_{11} \theta_1 = 0 \quad (28)$$

$$\phi_{1zz} - l_{12} \phi_1 = 0 \quad (29)$$

Subject to zeroth and firstorder boundary conditions are

$$\left. \begin{aligned} q_{0z} &= \alpha\sigma q_0, \theta_0 = 1, \phi_0 = 1 & \text{at } z &= \frac{1}{2} \\ q_{0z} &= \alpha\sigma q_0, \theta_0 = 0, \phi_0 = 0 & \text{at } z &= -\frac{1}{2} \end{aligned} \right\} \quad (30)$$

$$\left. \begin{aligned} q_{1z} &= \alpha\sigma q_1, \theta_1 = 1, \phi_1 = 1 & \text{at } z &= \frac{1}{2} \\ q_{1z} &= \alpha\sigma q_1, \theta_1 = 0, \phi_1 = 0 & \text{at } z &= -\frac{1}{2} \end{aligned} \right\} \quad (31)$$

The velocity, temperature, and concentration distributions are given by solving Equations (24)-(29) using the boundary conditions (30) and (31) correspondingly.

$$q_0 = \frac{2l_4}{l_3 - l_9} \frac{\text{Sinh}\left[\frac{\sqrt{l_9}}{2}\right]}{\text{Sinh}\sqrt{l_9}} \text{Cosh}[\sqrt{l_9}z] + \frac{2l_5}{l_3 - l_{11}} \frac{\text{Sinh}\left[\frac{\sqrt{l_{11}}}{2}\right]}{\text{Sinh}\sqrt{l_{11}}} \text{Cosh}[\sqrt{l_{11}}z] \quad (32)$$

$$q_1 = \frac{2l_4}{l_3 - l_{10}} \frac{\text{Sinh}\left[\frac{\sqrt{l_{10}}}{2}\right]}{\text{Sinh}\sqrt{l_{10}}} \text{Cosh}[\sqrt{l_{10}}z] + \frac{2l_5}{l_3 - l_{12}} \frac{\text{Sinh}\left[\frac{\sqrt{l_{12}}}{2}\right]}{\text{Sinh}\sqrt{l_{12}}} \text{Cosh}[\sqrt{l_{12}}z] \quad (33)$$

$$\theta_0 = 2 \frac{\text{Sinh}\left[\frac{\sqrt{l_9}}{2}\right]}{\text{Sinh}\sqrt{l_9}} \text{Cosh}[\sqrt{l_9}z] \quad (34)$$

$$\theta_1 = 2 \frac{\text{Sinh}\left[\frac{\sqrt{l_{10}}}{2}\right]}{\text{Sinh}\sqrt{l_{10}}} \text{Cosh}[\sqrt{l_{10}}z] \quad (35)$$

$$\phi_0 = 2 \frac{\text{Sinh}\left[\frac{\sqrt{l_{11}}}{2}\right]}{\text{Sinh}\sqrt{l_{11}}} \text{Cosh}[\sqrt{l_{11}}z] \quad (36)$$

$$\phi_1 = 2 \frac{\text{Sinh}\left[\frac{\sqrt{l_{12}}}{2}\right]}{\text{Sinh}\sqrt{l_{12}}} \text{Cosh}[\sqrt{l_{12}}z] \quad (37)$$

$$\text{where, } l_1 = 1 + \frac{1}{\beta_c}, l_2 = M^2(\beta_I + i\beta_{II}) + 2iR + \sigma^2, l_3 = \frac{l_2}{l_1}, l_4 = \frac{Gr \cos[\alpha]}{l_1}, l_5 = \frac{Gm \cos[\alpha]}{l_1}$$

$$l_6 = \frac{\text{Re}(i\omega + l_2)}{l_1}, l_9 = NPr, l_{10} = Pr(\text{Re } i\omega + l_9), l_{11} = Kr Sc, l_{12} = Sc(\text{Re } i\omega + Kr)$$

At the plate $z = \pm \frac{1}{2}$ the non-dimensional skin friction is given by[37]

$$\tau = -\frac{\partial q}{\partial z}\bigg|_{z=-\frac{1}{2}} = \frac{e^{i\pi t} \sqrt{l_{10}} l_4 \varepsilon \operatorname{Sech}\left[\frac{\sqrt{l_{10}}}{2}\right] \operatorname{Sinh}\left[\sqrt{l_{10}} z\right]}{l_{10} - l_3} + \frac{\sqrt{l_{11}} l_5 \operatorname{Sech}\left[\frac{\sqrt{l_{11}}}{2}\right] \operatorname{Sinh}\left[\sqrt{l_{11}} z\right]}{l_{11} - l_3} + \frac{\sqrt{l_{12}} l_5 \varepsilon \operatorname{Sech}\left[\frac{\sqrt{l_{12}}}{2}\right] \operatorname{Sinh}\left[\sqrt{l_{12}} z\right]}{l_{12} - l_3} + \frac{\sqrt{l_9} l_4 \operatorname{Sech}\left[\frac{\sqrt{l_9}}{2}\right] \operatorname{Sinh}\left[\sqrt{l_9} z\right]}{l_9 - l_3},$$

According to Fourier's law of heat conduction, the rate of heat transfer at the plate is represented in terms of the Nusselt number. [38]

$$Nu = \frac{\partial \theta}{\partial z}\bigg|_{z=-\frac{1}{2}} = -e^{i\pi t} \sqrt{l_{10}} \varepsilon \operatorname{Sech}\left[\frac{\sqrt{l_{10}}}{2}\right] \operatorname{Sinh}\left[\sqrt{l_{10}} z\right] - \sqrt{l_9} \operatorname{Sech}\left[\frac{\sqrt{l_9}}{2}\right] \operatorname{Sinh}\left[\sqrt{l_9} z\right],$$

The relation gives the rate of concentration in terms of Sherwood number.

$$Sh = \frac{\partial \phi}{\partial z}\bigg|_{z=-\frac{1}{2}} = -e^{i\pi t} \sqrt{l_{12}} \varepsilon \operatorname{Sech}\left[\frac{\sqrt{l_{12}}}{2}\right] \operatorname{Sinh}\left[\sqrt{l_{12}} z\right] - \sqrt{l_{11}} \operatorname{Sech}\left[\frac{\sqrt{l_{11}}}{2}\right] \operatorname{Sinh}\left[\sqrt{l_{11}} z\right]$$

4. Results and Discussion

Different parameters and their consequences are examined on MHD Casson fluid electrically conducting incompressible, rotating and radiating through two verticals in a porous medium. The exact values for Governing equations are resolved by using perturbation method. Figs 2 – 10 are the clear cut graphs to grasp the profiles of velocity, temperature and concentration. Different values of squared Hartmann number (M), dimensionless fluid concentration (ϕ), chemical reaction parameter (Kc) and resultant of thermal radiation parameter and heat source/sink parameter(N) are the profiles of velocity. These are shown in the fig 2(a) – 2(d). The interpretation of velocity components U and V are drawn in fig 2(a) – 2(d). The transient fluid velocity component U diminishes and velocity component V increases when the M, ϕ , Kc, N values are mounting. For fig 2(c) and 2 (d) boundary layer thickness varies in the region and fig 2(a) and 2(b) boundary layer thickness be as it starts.

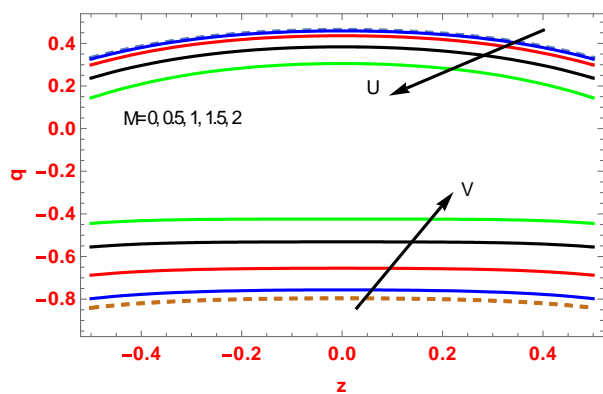
Fig 3(a) – 3(d) illustrate the consequences of velocity U and velocity V. The velocity U and the velocity V are diminishing with escalate in Casson parameter (β_c), rotation parameter(R), Schmidt number (Sc) and thermal Grashof number (Gr) in the area. In the fluid medium, the fluid velocity decreases by the inclination. Fig 4(a) – 4(c) portray the significance of hall parameter (α_i), ion slip parameter (α_e) and mass Grashof number (Gm) about the fluid velocity U and fluid velocity V. The fluid velocity U augments at the same time mass Grashof number (Gm), hall parameter (α_e) and ion slip parameter (α_i) are also increases. And the fluid velocity V decreases with the increase in the mass Grashof number(Gm), hall parameter (α_e) and ion slip parameter (α_i).

Fig 5 depicts the temperature profile at the boundary. The effect of Prandtl number increases when the temperature decreases. Also, boundary layer thickness reduces when the Prandtl number increases. Fig 6 displays the resultant of thermal radiation parameter and heat source/sink parameter(N) on the temperature profile. The temperature augments when the values of resultant of thermal radiation parameter and heat source/sink parameter (N) also increase. Also, it outcomes in increasing temperature within boundary layer. Fig 7(a) and fig 7(b) are exhibited the flow in the concentration profile. Concentration profile decreases when the chemical reaction parameter (Kc) and Schmidt number (Sc) increase. Thus boundary layer thickness reduces significantly. From Fig 8(a) and 8(b), The ratio of the convective mass transfer to the rate of diffusive mass transport Sherwood number (Sh) to the upper wall increases with increasing different values of Schmidt number (Sc) and Chemical reaction parameter (Kc) at time t also with distance $z = \pm \frac{1}{2}$. From Fig 9(a) and 9(b), the ratio between heat transfer by convection and heat transfer by conduction Nusselt number (Nu) increases with increasing Schmidt number (Sc) and Prandtl number (Pr) and time t where as it increases in negative region and decreases in the positive region. From Fig 10(a) and 10(b), an increase in the shear stress(τ) with increasing Casson parameter (β_c) and rotation parameter (R) and with respect to the time (t) whereas the parameters increase in the negative region and decrease in the positive region.

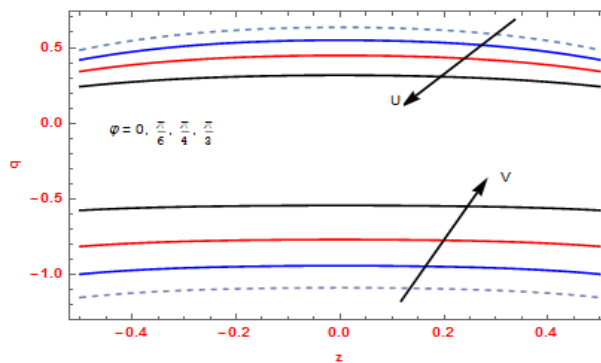
From table 1, It is observed that the Skin friction τ augments in the negative region and declines with the increase in Hartmann number, porous parameter, Thermal Grashof number, Prandtl number, dimensionless fluid concentration and Thermal conductivity in the positive region. The Stress constituent τ diminishes in the negative region and τ amplifies with an increase in Hall and ion

slip parameters in the positive region. Hence Hartmann number, porous parameter, thermal Grashof number, hall and ion slip parameter, Prandtl number, dimensionless fluid concentration and thermal conductivity parameter have an opposite consequence for the positive and negative regions. The Stress constituent τ increase with an increase in Casson parameter and time in the negative region and it has fluctuation in the positive region. The shear stress in both locations changed as the mass Grashof number and Schmidt number increased.

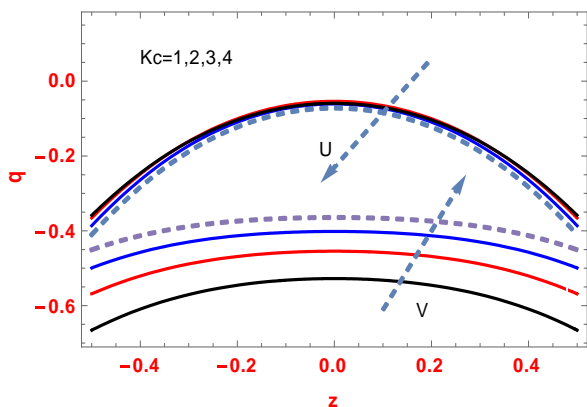
From the second table An rise in the Prandtl number, the radiation parameter, and the Nusselt numbers will follow. In the negative region, it is also diminished when the frequency of oscillations or time increases, but in the positive region, it is reduced as the parameters grow and numerous oscillations occur only in time. Table 3 shows the results. A rise in Schmidt number and thermal conductivity precedes an elevation in Sherwood number. In the negative zone, this is additionally augmented by an increase in the frequency of fluctuation in the radiation parameter and time, whereas in the positive region, the Sherwood number decreases with the thermal conductivity and fluctuation in the remaining parameters.



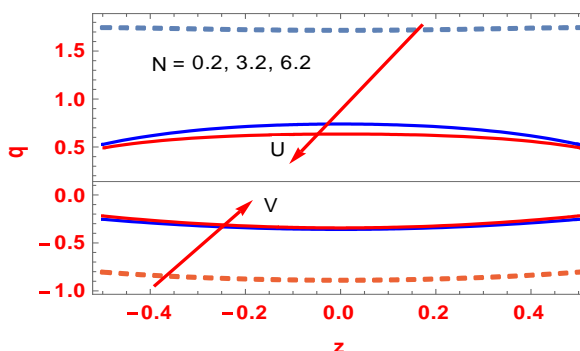
2 (a)



2 (b)

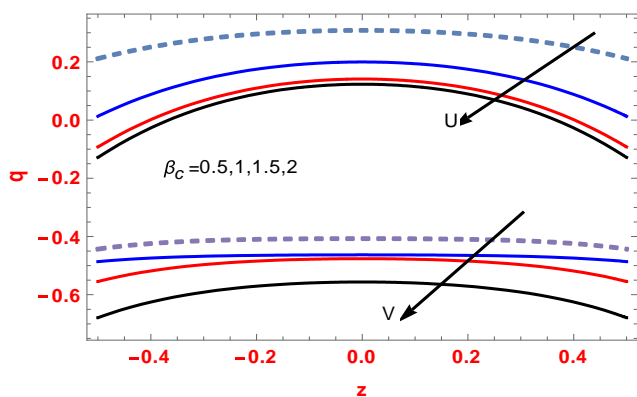


2 (c)

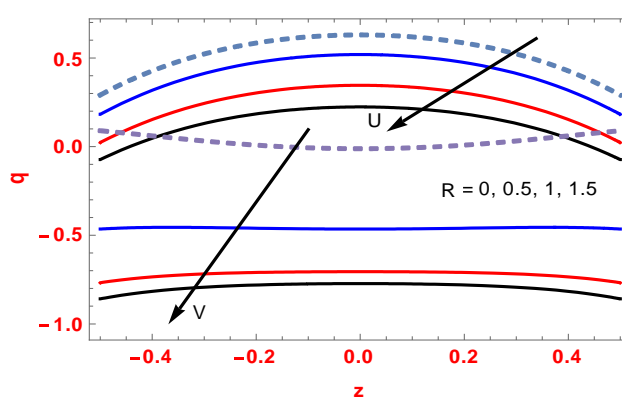


2 (d)

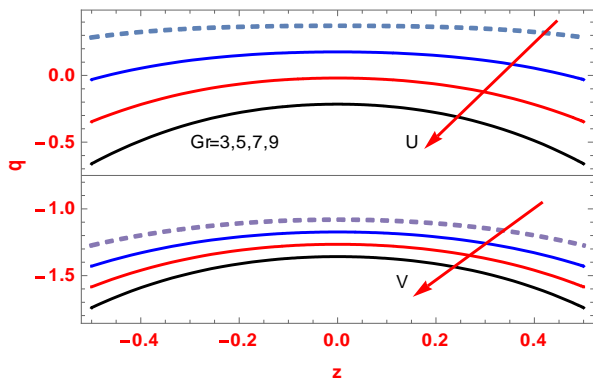
Fig. 2 (a) –2(d) The Velocity Profiles with M, ϕ , Kc and N



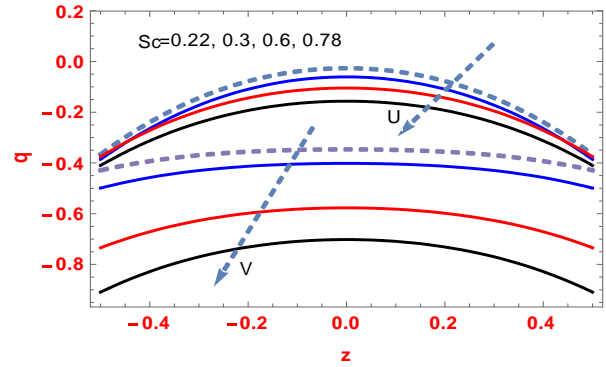
3 (a)



3 (b)

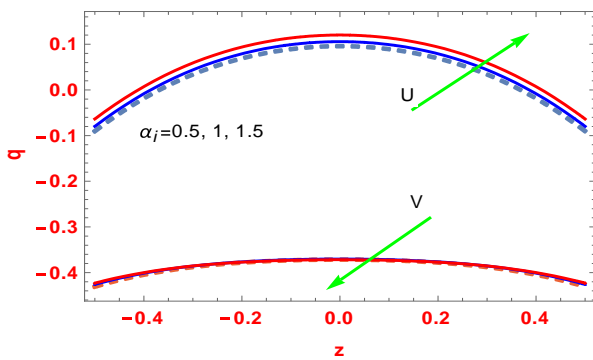


3 (c)

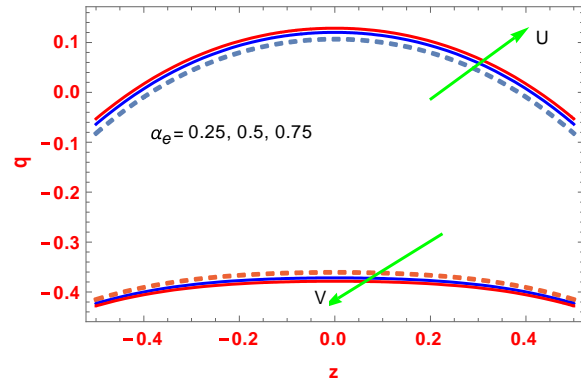


3 (d)

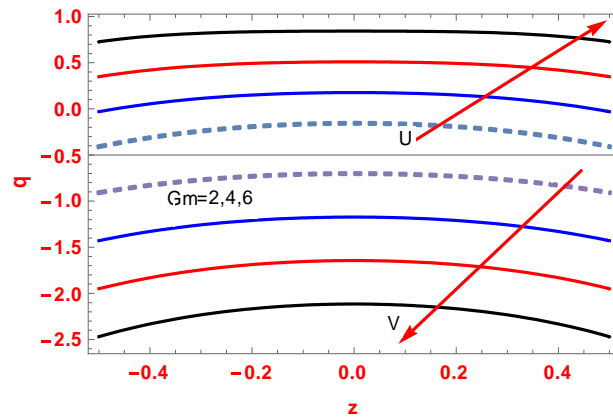
Fig. 3 (a) –3(d) The Velocity Profiles with β_c , R, Gr and Sc



4 (a)



4 (b)



4 (c)

Fig. 4 (a) – 4(c) The Velocity Profiles with α_f , α_e and Gm

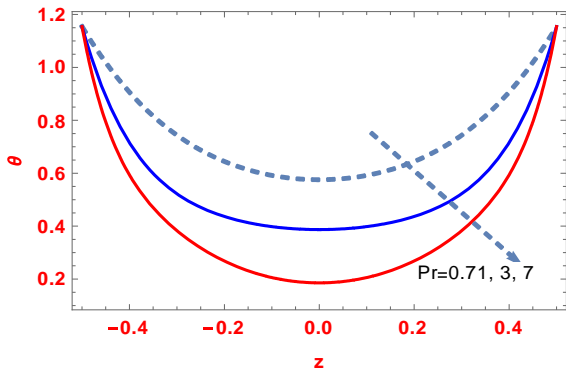


Fig. 5 The temperature profile with Pr

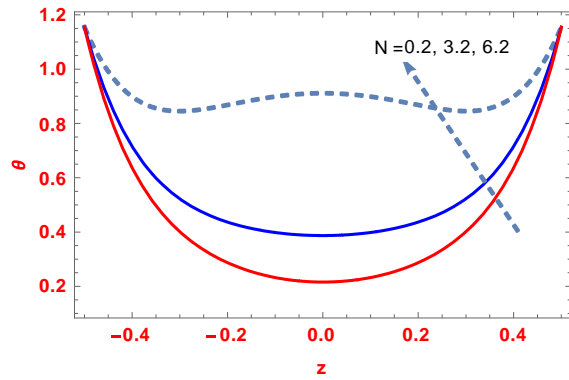
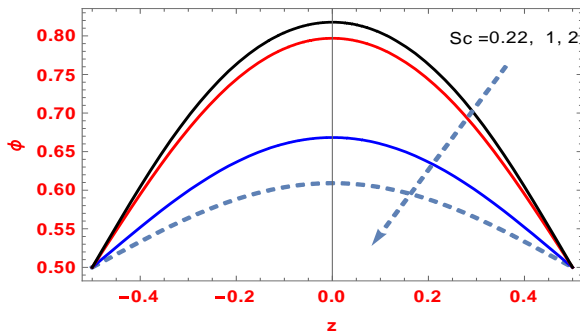
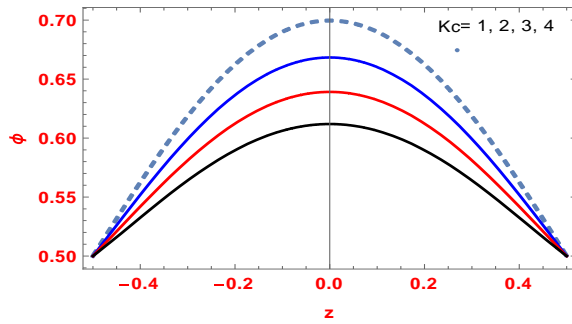


Fig. 6 The temperature profile with N

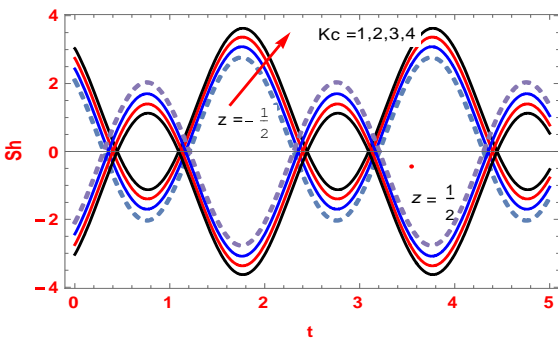


7 (a)

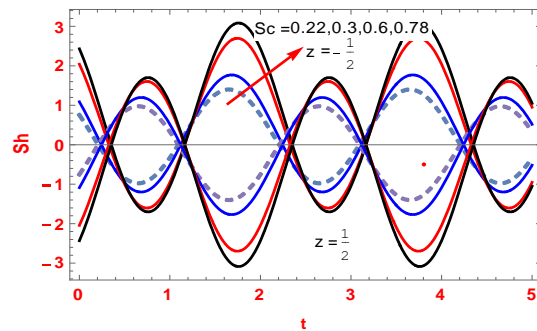


7 (b)

Fig. 7 (a) – 7(b) The Concentration profile with Sc and Kc

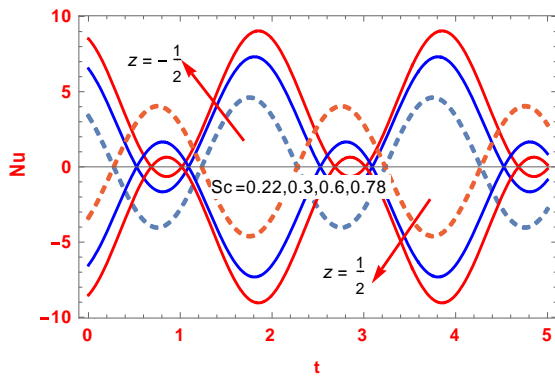


8 (a)

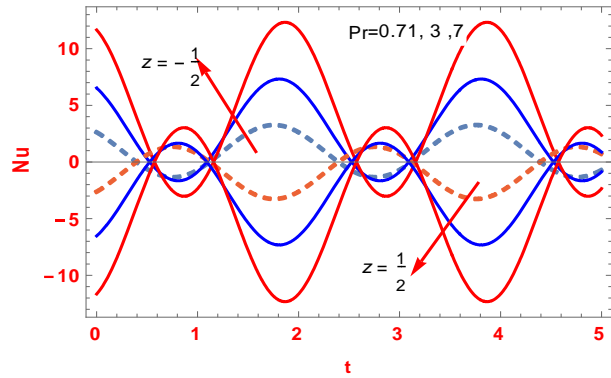


8 (b)

Fig. 8 (a) – 8(b) Sherwood number with Kc and Sc

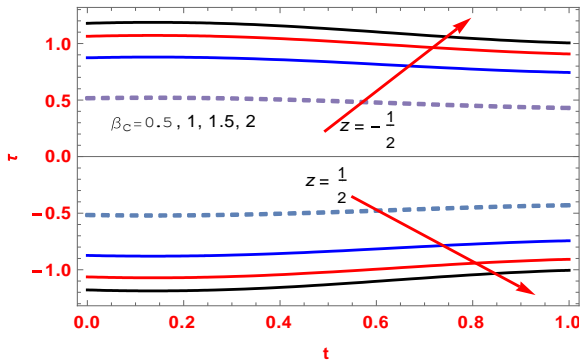


9 (a)

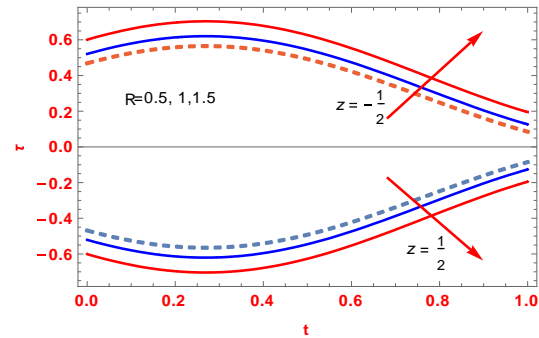


9 (b)

Fig. 9 (a) – 9(b) Nusselt number with Sc and Pr



10 (a)



10 (b)

Fig. 10 (a) –10(b) Shear stress with β_c and R

Table.1. Skin friction $z = \mu \frac{1}{2}, Ra = 1, \alpha = 0.5, \varepsilon = 0.001$

| M | σ | Gr | Gm | β_c | α_e | α_i | Pr | φ | Kr | Sc | t | τ |
|-----|----------|----|----|-----------|------------|------------|-----|-----------|----|------|-----|----------------|
| 0.5 | 0.5 | 5 | 4 | 0.5 | 0.2 | 2 | 0.7 | $\pi/6$ | 1 | 0.22 | 0.2 | μ 0.541693 |
| 1 | | | | | | | | | | | | μ 0.456041 |
| 1.5 | | | | | | | | | | | | μ 0.369738 |
| 2 | | | | | | | | | | | | μ 0.333455 |
| | 1 | | | | | | | | | | | μ 0.317453 |
| | 1.5 | | | | | | | | | | | μ 0.29557 |
| | | 7 | | | | | | | | | | μ 0.275016 |
| | | 9 | | | | | | | | | | μ 0.254462 |
| | | | 6 | | | | | | | | | μ 0.427939 |
| | | | 8 | | | | | | | | | μ 0.601416 |
| | | | | 1 | | | | | | | | μ 0.792899 |
| | | | | 1.5 | | | | | | | | μ 0.793522 |
| | | | | 2 | | | | | | | | μ 0.748224 |
| | | | | | 0.4 | | | | | | | μ 0.939231 |
| | | | | | 0.6 | | | | | | | μ 1.07336 |
| | | | | | 0.8 | | | | | | | μ 1.16694 |

- ✦ The Sherwood number representing the transport from a moving fluid to a vertical plate with the chemical reaction parameter and Schmidt number are given the rate of mass transport near the plate with an increase in time.
- ✦ Nusselt number and shear stress are examined over channel distance $\pm \frac{d}{2}$. The resolution of the convection in the near wall negative region heat and force lead to increment in the thickness and positive region heat and force lead to decrement in the thickness.
- ✦ The present model shows the flow of non-Newtonian fluid through porous medium by means of Hall and ion slip impacts portrays the augmentation.

References

- [1] B. B. Mallik, "A Mathematical Analysis On Blood Flow Through ϕ hj § aÑ p j l," no. 1, pp. 707–716, 2011.
- [2] G. O. H. M. S. Law, "Magnetic Reconnection Solutions Based on a," *Sol. Phys.*, pp. 131–150, 2003.
- [3] A. A. Dar and K. Elangovan, "Effect of magnetic field and rotation on the micropolar fluid model of blood flow through stenotic arteries," *Int. J. Biomed. Eng. Technol.*, vol. 26, no. 2, pp. 171–185, 2018, doi: 10.1504/IJBET.2018.089310.
- [4] F. Ali, A. Imtiaz, I. Khan, and N. A. Sheikh, "Flow of magnetic particles in blood with isothermal heating: A fractional model for two-phase flow," *J. Magn. Magn. Mater.*, vol. 456, pp. 413–422, 2018, doi: 10.1016/j.jmmm.2018.02.063.
- [5] M. Saqib, I. Khan, and S. Shafie, "Generalized magnetic blood flow in a cylindrical tube with magnetite dusty particles," *J. Magn. Magn. Mater.*, vol. 484, pp. 490–496, 2019, doi: 10.1016/j.jmmm.2019.03.032.
- [6] K. Ramakrishnan, "Studies of blood flow through porous medium with slip effects," *AIP Conf. Proc.*, vol. 2095, no. April, 2019, doi: 10.1063/1.5097532.
- [7] S. A. Shehzad, T. Hayat, M. Qasim, and S. Asghar, "Effects of mass transfer on MHD flow of Casson fluid with chemical reaction and suction," *Brazilian J. Chem. Eng.*, vol. 30, no. 1, pp. 187–195, 2013, doi: 10.1590/S0104-66322013000100020.
- [8] A. Hussanan, M. Z. Salleh, R. M. Tahar, and I. Khan, "Unsteady boundary layer flow and heat transfer of a Casson fluid past an oscillating vertical plate with Newtonian heating," *PLoS One*, vol. 9, no. 10, 2014, doi: 10.1371/journal.pone.0108763.
- [9] A. Khalid, I. Khan, A. Khan, and S. Shafie, "Unsteady MHD free convection flow of Casson fluid past over an oscillating vertical plate embedded in a porous medium," *Eng. Sci. Technol. an Int. J.*, vol. 18, no. 3, pp. 309–317, 2015, doi: 10.1016/j.jestch.2014.12.006.
- [10] S. A. Shehzad, T. Hayat, and A. Alsaedi, "Three-dimensional MHD flow of casson fluid in porous medium with heat generation," *J. Appl. Fluid Mech.*, vol. 9, no. 1, pp. 215–223, 2016, doi: 10.18869/acadpub.jafm.68.224.24042.
- [11] R. Biswas, M. Mondal, D. Sarkar, and S. Ahmmed, "Effects of Radiation and Chemical Reaction on MHD Unsteady Heat and Mass Transfer of Casson Fluid Flow Past a Vertical Plate," *J. Adv. Math. Comput. Sci.*, vol. 23, no. 2, pp. 1–16, 2017, doi: 10.9734/jamcs/2017/34292.
- [12] A. Hussanan, M. Z. Salleh, I. Khan, and R. M. Tahar, "Heat transfer in magnetohydrodynamic flow of a casson fluid with porous medium and newtonian heating," *J. Nanofluids*, vol. 6, no. 4, pp. 784–793, 2017, doi: 10.1166/jon.2017.1359.
- [13] K. A. Abro and I. Khan, "Analysis of the heat and mass transfer in the MHD flow of a generalized Casson fluid in a porous space via non-integer order derivatives without a singular kernel," *Chinese J. Phys.*, vol. 55, no. 4, pp. 1583–1595, 2017, doi: 10.1016/j.cjph.2017.05.012.
- [14] J. R. Pattnaik, G. C. Dash, and S. Singh, "Radiation and mass transfer effects on MHD flow through porous medium past an exponentially accelerated inclined plate with variable temperature," *Ain Shams Eng. J.*, vol. 8, no. 1, pp. 67–75, Mar. 2017, doi: 10.1016/j.asej.2015.08.014.
- [15] M. Saqib, F. Ali, I. Khan, and N. A. Sheikh, "Heat and mass transfer phenomena in the flow of Casson fluid over an infinite oscillating plate in the presence of first-order chemical reaction and slip effect," *Neural Comput. Appl.*, vol. 30, no. 7, pp. 2159–2172, 2018, doi: 10.1007/s00521-016-2810-x.
- [16] M. Veerakrishna, G. Subba Reddy, and A. J. Chamkha, "Hall effects on unsteady MHD oscillatory free convective flow of second grade fluid through porous medium between two vertical plates," *Phys. Fluids*, vol. 30, no. 2, 2018, doi: 10.1063/1.5010863.
- [17] D. Khan, A. Khan, I. Khan, F. Ali, F. ul Karim, and I. Tlili, "Effects of Relative Magnetic Field, Chemical Reaction, Heat Generation and Newtonian Heating on Convection Flow of Casson Fluid over a Moving Vertical Plate Embedded in a Porous Medium," *Sci. Rep.*, vol. 9, no. 1, pp. 1–18, 2019, doi: 10.1038/s41598-018-36243-0.
- [18] K. V. B. Rajakumar, K. S. Balamurugan, C. V. Ramana Murthy, and N. Ranganath, "Radiation, dissipation, and dufour effects on MHD free convection flow through a vertical oscillatory porous plate with ion slip current," *Lect. Notes Mech. Eng.*, vol. 36, no. 2, pp. 587–596, 2019, doi: 10.1007/978-981-13-1903-7_67.
- [19] B. K. Jha and M. N. Sarki, "Chemical reaction and Dufour effects on nonlinear free convection heat and mass transfer flow near a vertical moving porous plate," no. June, pp. 1–16, 2019, doi: 10.1002/htj.21649.

- [20] S. Kumar and S. Vishwanath, "Hall and ion-slip effects on MHD free convective flow of a viscoelastic fluid through porous regime in an inclined channel with moving magnetic field," *Kragujev. J. Sci.*, vol. 42, no. 42, pp. 5–18, 2020, doi: 10.5937/kgjsci2042005k.
- [21] C. R. Makhalemele, L. Rundora, and S. O. Adesanya, "Mixed Convective Flow of Unsteady Hydromagnetic Couple Stress Fluid Through a Vertical Channel Filled with Porous Medium," *Int. J. Appl. Mech. Eng.*, vol. 25, no. 4, pp. 148–161, 2020, doi: 10.2478/ijame-2020-0055.
- [22] J. K. Singh and G. S. Seth, "Hydromagnetic free convective flow of Walters' -B fluid over a vertical surface with time varying surface conditions," vol. 2, no. November 2019, pp. 295–307, 2020, doi: 10.1108/WJE-06-2019-0163.
- [23] M. V. Krishna and A. J. Chamkha, "Hall and ion slip effects on MHD Rotating Boundary layer flow of Nanofluid past an infinite vertical plate," *Results Phys.*, p. 102652, 2019, doi: 10.1016/j.rinp.2019.102652.
- [24] M. V. Krishna, "Hall and ion slip impacts on unsteady MHD free convective rotating flow of Jeffreys fluid with ramped wall temperature," *Int. Commun. Heat Mass Transf.*, vol. 119, p. 104927, 2020, doi: 10.1016/j.icheatmasstransfer.2020.104927.
- [25] M. V. Krishna, C. S. Sravanthi, R. Subba, and R. Gorla, "Hall and ion slip effects on MHD rotating flow of ciliary propulsion of microscopic organism through porous media," *Int. Commun. Heat Mass Transf.*, vol. 112, p. 104500, 2020, doi: 10.1016/j.icheatmasstransfer.2020.104500.
- [26] M. V. Krishna and A. J. Chamkha, "Hall and ion slip effects on MHD rotating flow of elastico-viscous fluid through porous medium," *Int. Commun. Heat Mass Transf.*, vol. 113, p. 104494, 2020, doi: 10.1016/j.icheatmasstransfer.2020.104494.
- [27] M. V. Krishna, N. A. Ahamad, and A. J. Chamkha, "Hall and ion slip impacts on unsteady MHD convective rotating flow of heat generating / absorbing second grade fluid," *Alexandria Eng. J.*, 2020, doi: 10.1016/j.aej.2020.10.013.
- [28] M. V. Krishna, "Hall and ion slip effects on MHD free convective rotating flow bounded by the semi - infinite vertical porous surface," *Heat Transf.*, no. November 2019, pp. 1–19, 2020, doi: 10.1002/htj.21700.
- [29] G. Dharmiah, W. Sridhar, K. S. Balamurugan, and K. C. Kala, "Hall and Ion Slip Impact on Magneto-Titanium Alloy Nanoliquid with Diffusion Thermo and Radiation Absorption," *Int. J. Ambient Energy*, vol. 0, no. 0, pp. 1–30, 2020, doi: 10.1080/01430750.2020.1831597.
- [30] M. Veera Krishna, N. Ameer Ahamad, and A. F. Aljohani, "Thermal radiation, chemical reaction, Hall and ion slip effects on MHD oscillatory rotating flow of micro-polar liquid," *Alexandria Eng. J.*, vol. 60, no. 3, pp. 3467–3484, 2021, doi: 10.1016/j.aej.2021.02.013.
- [31] M. Venkateswarlu and P. Bhaskar, "Mathematical Study of Imposed Magnetic Field on Radiative Hydromagnetic Casson Fluid Flow in a Micro-Channel with Asymmetric Heating," *J. Nanofluids*, vol. 10, no. 4, pp. 478–490, 2021, doi: 10.1166/jon.2021.1810.
- [32] G. Dharmiah, W. Sridhar, K. S. Balamurugan, and K. Chandra Kala, "Hall and ion slip impact on magneto-titanium alloy nanoliquid with diffusion thermo and radiation absorption," *Int. J. Ambient Energy*, 2020, doi: 10.1080/01430750.2020.1831597.
- [33] W. G. England and A. F. Emery, "Thermal radiation effects on the laminar free convection boundary layer of an absorbing gas," *J. Heat Transfer*, vol. 91, no. 1, pp. 37–44, 1969, doi: 10.1115/1.3580116.
- [34] M. Veera Krishna, N. Ameer Ahamad, and A. J. Chamkha, "Hall and ion slip effects on unsteady MHD free convective rotating flow through a saturated porous medium over an exponential accelerated plate," *Alexandria Eng. J.*, vol. 59, no. 2, pp. 565–577, 2020, doi: 10.1016/j.aej.2020.01.043.
- [35] N. H. Baker, "Variable Stars," *Ann. N. Y. Acad. Sci.*, vol. 187, no. 1, pp. 207–212, 1972, doi: 10.1111/j.1749-6632.1972.tb48329.x.
- [36] T. Hayat, S. Asghar, A. Tanveer, and A. Alsaedi, "Effects of Hall current and ion-slip on the peristaltic motion of couple stress fluid with thermal deposition," *Neural Comput. Appl.*, vol. 31, no. 1, pp. 117–126, 2019, doi: 10.1007/s00521-017-2984-x.
- [37] M. Ra and S. Nasrin, "Hall and Ion-Slip Currents Effects on Unsteady MHD Fluid Flow over an Inclined Plate with Inclined Magnetic Field and Variable Temperature Hall and Ion-Slip Currents Effects on Unsteady MHD Fluid Flow over an Inclined Plate with Inclined Magnetic Field an," 2021.
- [38] U. J. Das and M. Das, "Unsteady Mhd Rotating and Chemically Reacting Fluid Flow Over an Oscillating Vertical Surface in a Darcian Porous Regime," *Front. Heat Mass Transf.*, vol. 17, pp. 1–8, 2021, doi: 10.5098/hmt.17.18.
- [39] Hayat, T., Asghar, S., Tanveer, A. and Alsaedi, A., 2019. Effects of Hall current and ion-slip on the peristaltic motion of couple stress fluid with thermal deposition. *Neural Computing and Applications*, 31(1), pp.117-126.
- [40] Sutton, G.W. and Sherman, A. (1965) *Engineering Magnetohydrodynamics*. McGraw-Hill, New York.